Fracture behaviour of Cu–Zn–Co and Cu–Zn–Ni alloys during superplastic deformation

T. CHANDRA, I. UEBEL
Department of Metallurgy and Materials Engineering, University of Wollongong, Wollongong 2500, New South Wales, Australia

Cavitation and fracture behaviour in two commercial α/β brasses, one modified with 2 wt% Co (Cu–Zn–Co) and the other with 2 wt% Cr (Cu–Zn–Cr), have been investigated in Region II of superplastic flow. These alloying elements form cobalt-rich (0.3 μm average diameter) and chromium-rich (5 μm average diameter) precipitate particles which are distributed uniformly in the matrix and which play an important role in cavitation and inhibiting grain growth during deformation. Void size distributions, volume fraction of voids and the number of voids per unit area have been measured as a function of strain in Region II and the results show a very marked difference in the degree of cavitation in Cu–Zn–Co and Cu–Zn–Cr alloys. Experiments show that the deformation is quasi-uniform with little or no necking in the specimens of Cu–Zn–Co alloy in Region II, and the final fracture occurred by the growth and interlinkage of internal voids. On the other hand, in the specimens of Cu–Zn–Cr alloy a sharp or localized neck developed early in the deformation in Region II and the specimen pulled down to a fine point leading to failure by necking. The importance of diffusion or slip accommodation of grain boundary sliding in void formation during superplastic flow is discussed and a criterion for failure is suggested.

1. Introduction

It is now known that one of the problems which inhibit commercial exploitation of some superplastic materials is the formation of cavities during superplastic flow. Cavitation leads to a decrease in the amount of deformation achieved [1, 2] and can have an adverse effect on the ambient-temperature mechanical properties of superplastically formed products [3, 4].

An earlier study by Chandra and Uebel [5] examined the influence of cavitation at grain/phase boundaries and at precipitate particles on the tensile ductility of cobalt-modified (Cu–Zn–Co) and the chromium-modified (Cu–Zn–Cr) brasses during superplastic deformation. The major conclusions of the work were that both alloys attained tensile elongations between 170 and 220% in Region II of superplastic flow and had similar values of strain-rate sensitivity (m). These alloys cavitated during superplastic deformation but a marked difference in the degree of cavitation was observed in the specimens of Cu–Zn–Co and Cu–Zn–Cr, even though they exhibited very small difference in their flow stresses in Region II. The Cu–Zn–Co alloy cavitated extensively whilst a very few and small cavities were present in Cu–Zn–Cr specimens. In cobalt-modified specimens, the cavitation at a given strain peaked at a strain rate approximately equal to that corresponding to maximum m value while the extent of cavitation was minimum in chromium-modified alloy under these conditions.

Although no systematic investigation of the fracture process was carried out, visual and preliminary metallographic examination revealed a significant difference in their fracture behaviour. In view of the different cavitation levels observed in these alloys, one of the aims of this paper is to examine the differences in fracture processes of Cu–Zn–Co and Cu–Zn–Cr alloys in Region II of the superplastic flow by examining the surfaces of fractured specimens using scanning electron microscopy. The other objective is also to demonstrate that void formation depends on both the material and the test conditions.

2. Experimental procedure

Experiments were performed on the two α/β brasses with nominal additions of 2 wt % Cr and 2 wt % Co (supplied by Imperial Metals Industries, Birmingham, UK). The actual compositions of these alloys are given in Table I. The details of materials preparation and heat-treatment procedure to obtain the stable grain/phase size of 32 μm are given elsewhere [5]. Both Cu–Zn–Co and Cu–Zn–Cr are duplex in structure at the testing temperatures and contain a uniform dispersion of a cobalt-rich and chromium-rich precipitate phase, respectively, which inhibits grain growth

TABLE I Composition of Cu–Zn–Cr and Cu–Zn–Co alloys

Alloy	Composition (wt %)							
	Cu	Zn	Cr	Co	Bi	Pb	Sn	Cd
Cu–Zn–Cr	57.6	Rem	1.82	–	0.0002	0.01	0.03	0.05
Cu–Zn–Co	58.2	Rem	–	1.8	0.0002	0.01	0.03	0.05

0022–2461/88 $03.00 + .12

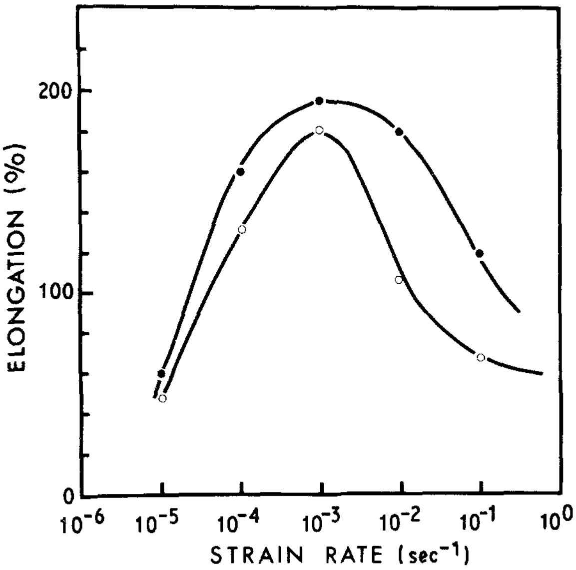

Figure 1 Tensile elongations to fracture against initial strain rate for (○) Cu–Zn–Co and (●) Cu–Zn–Cr alloys deformed at 785° C.

and thus facilitates the production of the stable grain sizes required for superplastic deformation.

Tensile specimens, having a gauge length of 16 mm and 16 mm^2 cross-sectional area, were machined from the cylindrical rods with the tensile axis parallel to the extruded direction. The specimens were tested on a screw-driven tensile machine operating at a constant rate of cross-head displacement. All tests were conducted in air at 785° C at an initial strain rate of 10^{-3} sec^{-1}, and prior to testing the specimens were allowed to equilibrate at the test temperature for 45 min. A steady temperature with a tolerance of $\pm 2°$ C was maintained by means of a three-zone split vertical furnace and a proportional temperature controller. Specimens were deformed to various strains and were cooled rapidly and sectioned along the gauge length for optical microscopy. The distribution of void sizes was determined from at least 1100 cavities measured for each specimen using the Johnson–Saltykov method [6]. Scanning electron microscopy was used to examine the fracture surfaces.

3. Results

Fig. 1 shows the variation of the tensile elongation at fracture with the initial strain rate for specimens of the Cu–Zn–Co and Cu–Zn–Cr alloys tested at a temperature of 785° C. The results indicate that at an intermediate strain rate of 10^{-3} sec^{-1} (in Region II), the Cu–Zn–Co and Cu–Zn–Cr alloys show maximum elongations of 170 and 200%, respectively. The appearance of the specimens after fracture is shown in Fig. 2. It can be seen that the specimen of Cu–Zn–Co alloys showed uniform deformation with little or no necking at fracture, that is to say it exhibited a non-ideal tensile fracture in which necking seems to be diffused rather than localized. On the other hand, the specimens of Cu–Zn–Cr alloy gradually pulled out to a fine point at fracture exhibiting an ideal type of fracture. These observations suggest that the neck formation is important in chromium-modified alloy in which deformation is confined primarily to the neck region.

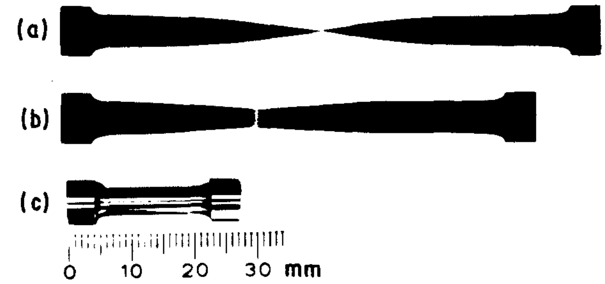

Figure 2 Tensile specimens deformed to failure at an initial strain rate of 10^{-3} sec^{-1} in Region II: (a) Cu–Zn–Cr, (b) Cu–Zn–Co, (c) untested tensile specimen.

A series of photomicrographs presented in Figs 3 and 4 shows typical areas within the gauge length of specimens of the alloys pulled to different strains at 785° C and an initial strain rate of 10^{-3} sec^{-1}. It can be seen that there is a marked difference in the degree of cavitation in the two alloy systems. The specimens of Cu–Zn–Co alloy showed substantial levels of cavitation with nucleation occurring early in the test. Both the number and size increased rapidly with strain and this is reflected in the histograms of void size plotted against number per unit area as shown in Fig 5a. Under identical deformation conditions, specimens of Cu–Zn–Cr alloy showed a few and very small cavities initially at low strains, and although the number of cavities increased as deformation continued, their growth was restricted as indicated by the results of Fig. 5b.

Fig. 6 shows that specimens of two alloys exhibited a significant difference in the area fraction of voids, A_v, which depends on both the number and size of voids. In specimens strained to an elongation of 140%, A_v was found to be less than 1% in the chromium alloy whilst the cobalt alloy exhibited a much higher ($> 18\%$) area fraction of voids A_v. These results further indicate that void growth was very much restricted in Cu–Zn–Cr specimens.

The fracture tips of specimens of two alloy systems tested to failure in Region II at 785° C are shown in Fig. 7. Extensive cavitation is evident near to the point of fracture in the Cu–Zn–Co specimen and there are many places with thin ligaments of material between voids. Large voids were present throughout the gauge length at points far removed from the fracture tip. There is a clear evidence for cavity interlinkage as can be seen in this figure. On the other hand, in specimens of Cu–Zn–Cr alloy very small cavities were present in the gauge length and even at the fracture tip large voids were not visible.

3.1. Fracture surfaces

Fig. 8 shows scanning electron micrographs of the fracture surfaces of specimens of the two alloys pulled to failure in Region II at 785° C. The surface of the Cu–Zn–Co alloy is uniformly covered with many small holes which do not vary greatly in size, (Fig. 8a). The fracture surface displays crests and troughs and its appearance indicates that the final fracture occurs by decohesion along interfaces weakened by cavitation. It is believed that the voids coalesce by internal

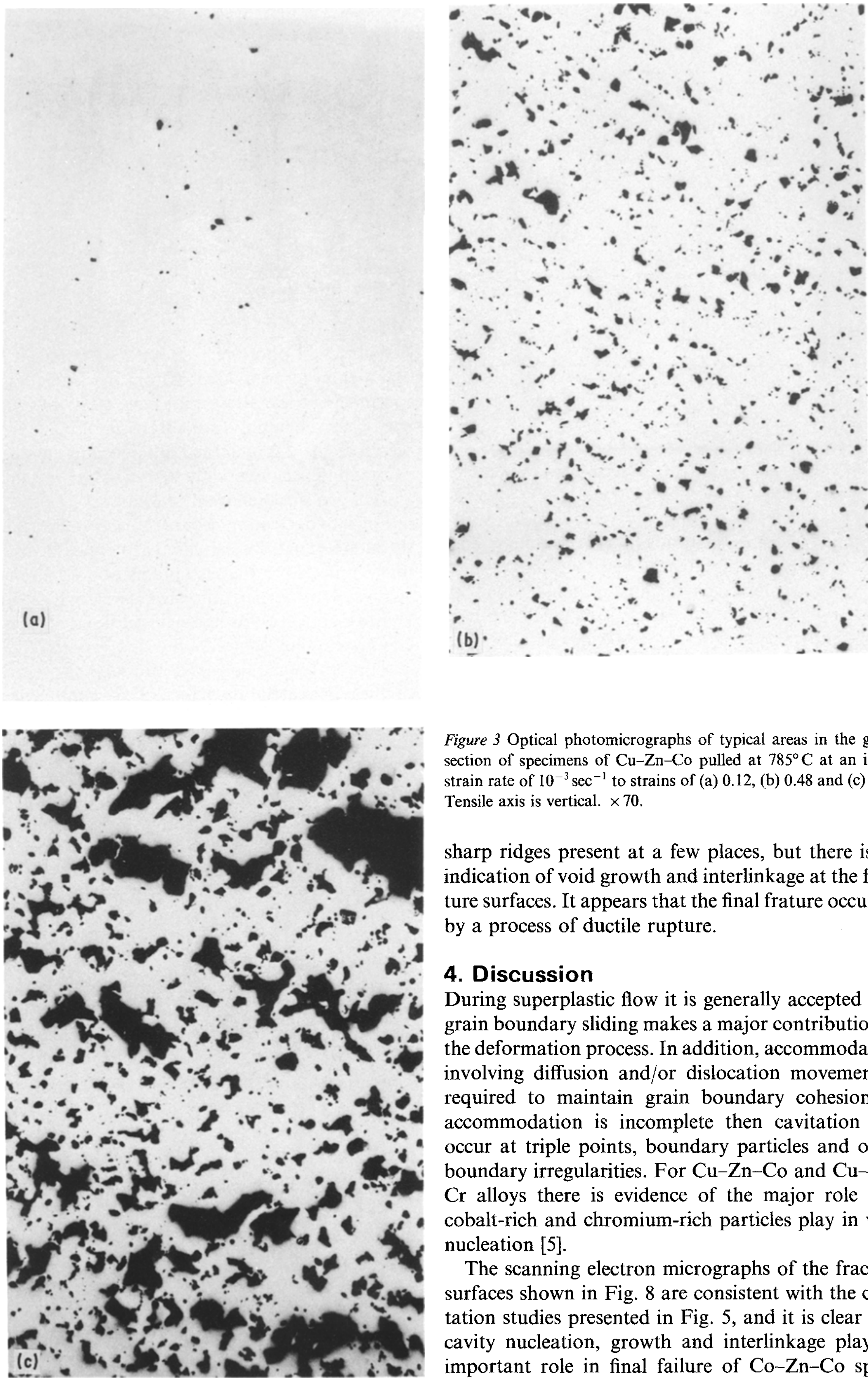

Figure 3 Optical photomicrographs of typical areas in the gauge section of specimens of Cu–Zn–Co pulled at 785° C at an initial strain rate of $10^{-3}\,sec^{-1}$ to strains of (a) 0.12, (b) 0.48 and (c) 1.24. Tensile axis is vertical. ×70.

necking, which results from tensile plastic instability in the ductile matrix between voids.

The fracture surfaces of the specimens of Cu–Zn–Cr alloy in Fig. 8b, on the other hand, show very few small holes at isolated places. The individual grains are visible over the entire surface and there were some sharp ridges present at a few places, but there is no indication of void growth and interlinkage at the fracture surfaces. It appears that the final frature occurred by a process of ductile rupture.

4. Discussion

During superplastic flow it is generally accepted that grain boundary sliding makes a major contribution to the deformation process. In addition, accommodation involving diffusion and/or dislocation movement is required to maintain grain boundary cohesion. If accommodation is incomplete then cavitation will occur at triple points, boundary particles and other boundary irregularities. For Cu–Zn–Co and Cu–Zn–Cr alloys there is evidence of the major role that cobalt-rich and chromium-rich particles play in void nucleation [5].

The scanning electron micrographs of the fracture surfaces shown in Fig. 8 are consistent with the cavitation studies presented in Fig. 5, and it is clear that cavity nucleation, growth and interlinkage play an important role in final failure of Co–Zn–Co specimens. In Cu–Zn–Co specimens, at the strain rate corresponding to maximum elongation in Region II, grain boundary sliding seems to be an important deformation process and this gives rise to very large number of internal cavities associated with cobalt-rich precipitate particles. Fleck *et al.* [7], in their work on a copper-base alloy, have reported that the particles

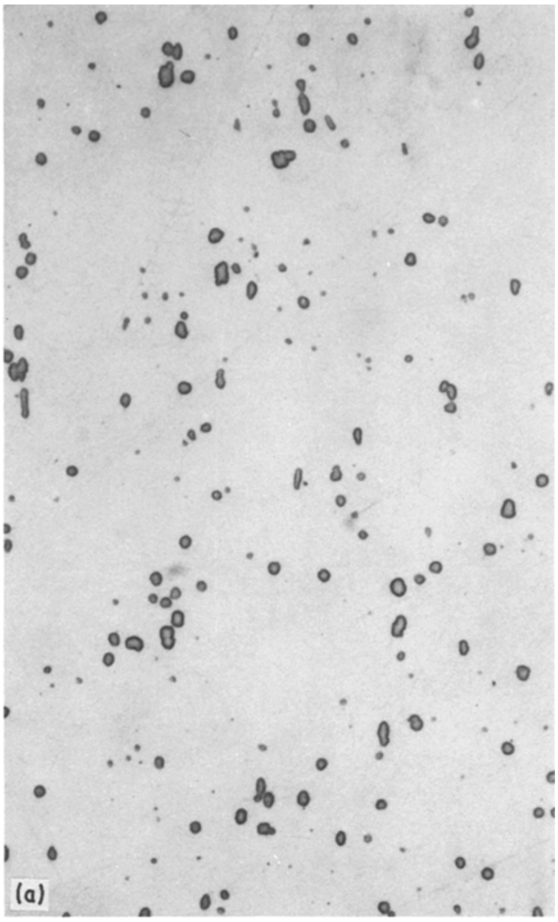

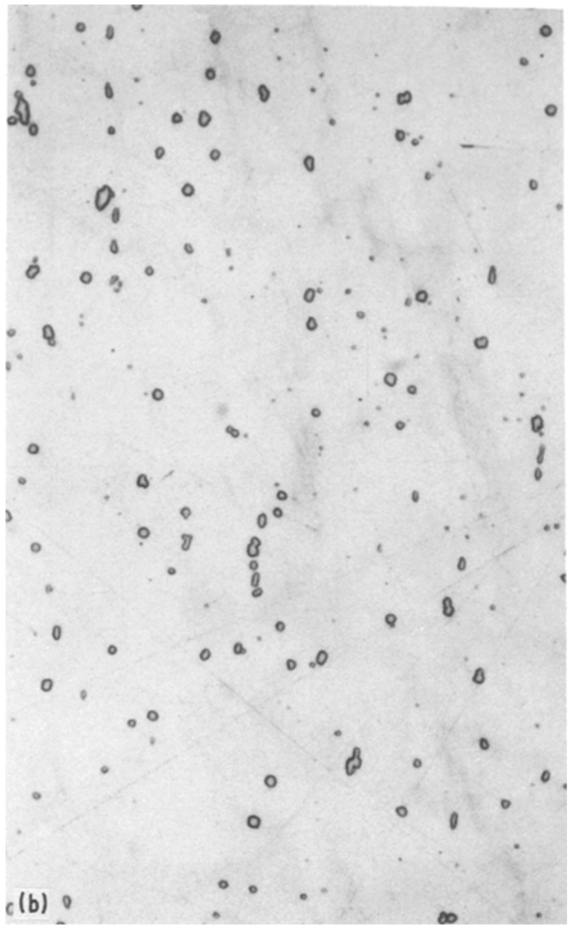

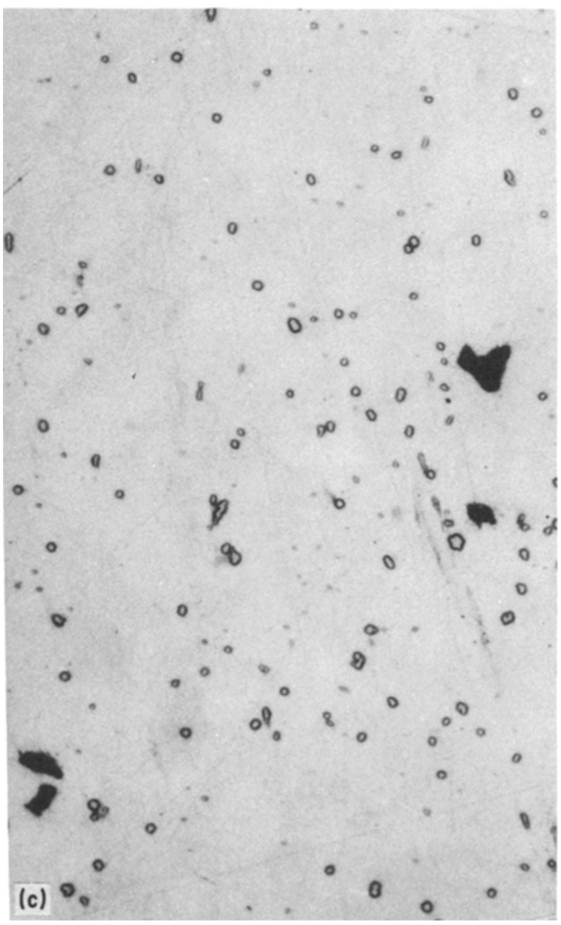

Figure 4 Optical photomicrographs of typical areas in the gauge section of specimens of Cu–Zn–Cr pulled at 785° C at an initial strain rate of $10^{-3} sec^{-1}$ to strains of (a) 0.10, (b) 0.46 and (c) 1.35. Tensile axis is vertical. ×280.

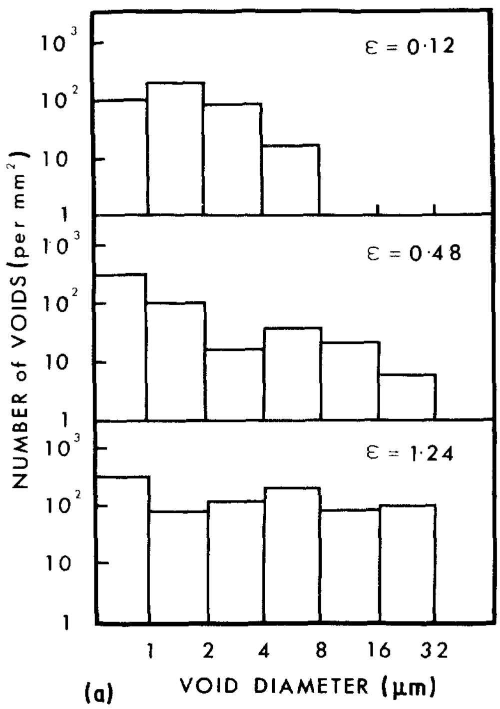

Figure 5 Histograms showing the number of voids against void size in specimens of (a) Cu–Zn–Co corresponding to the micrographs in Fig. 3 and (b) Cu–Zn–Cr corresponding to the micrographs in Fig. 4.

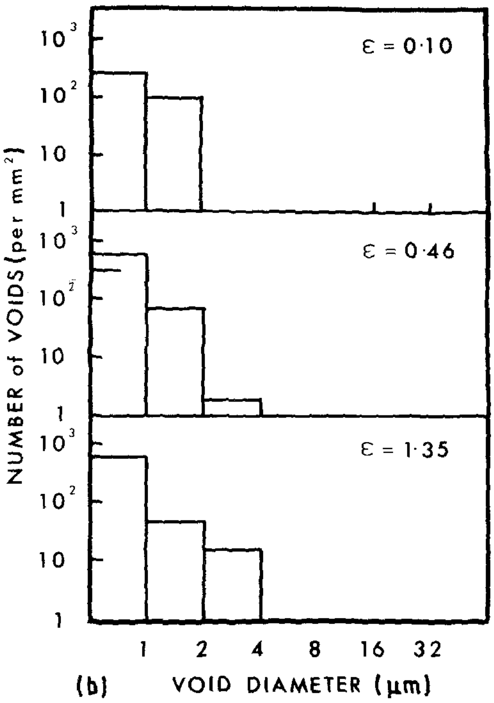

Figure 5 Continued.

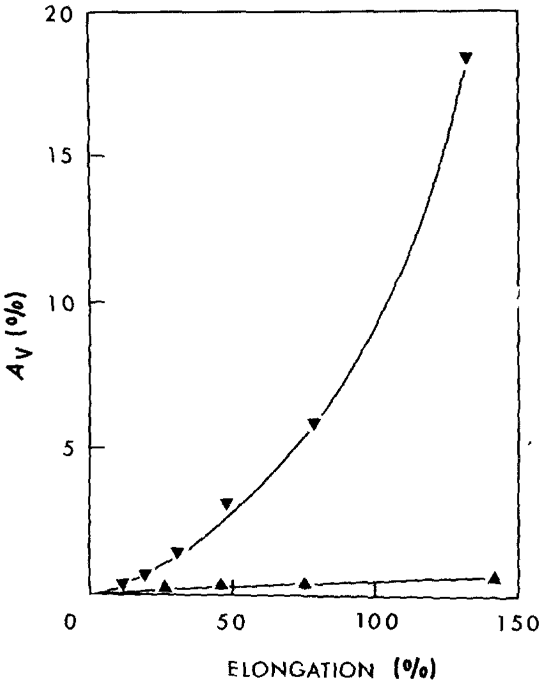

Figure 6 Showing the change in the total area fraction of voids A_v with elongation in specimens of (▼) Cu–Zn–Co and (▲) Cu–Zn–Cr alloys pulled at an initial strain rate of $10^{-3}\,sec^{-1}$ at 785° C.

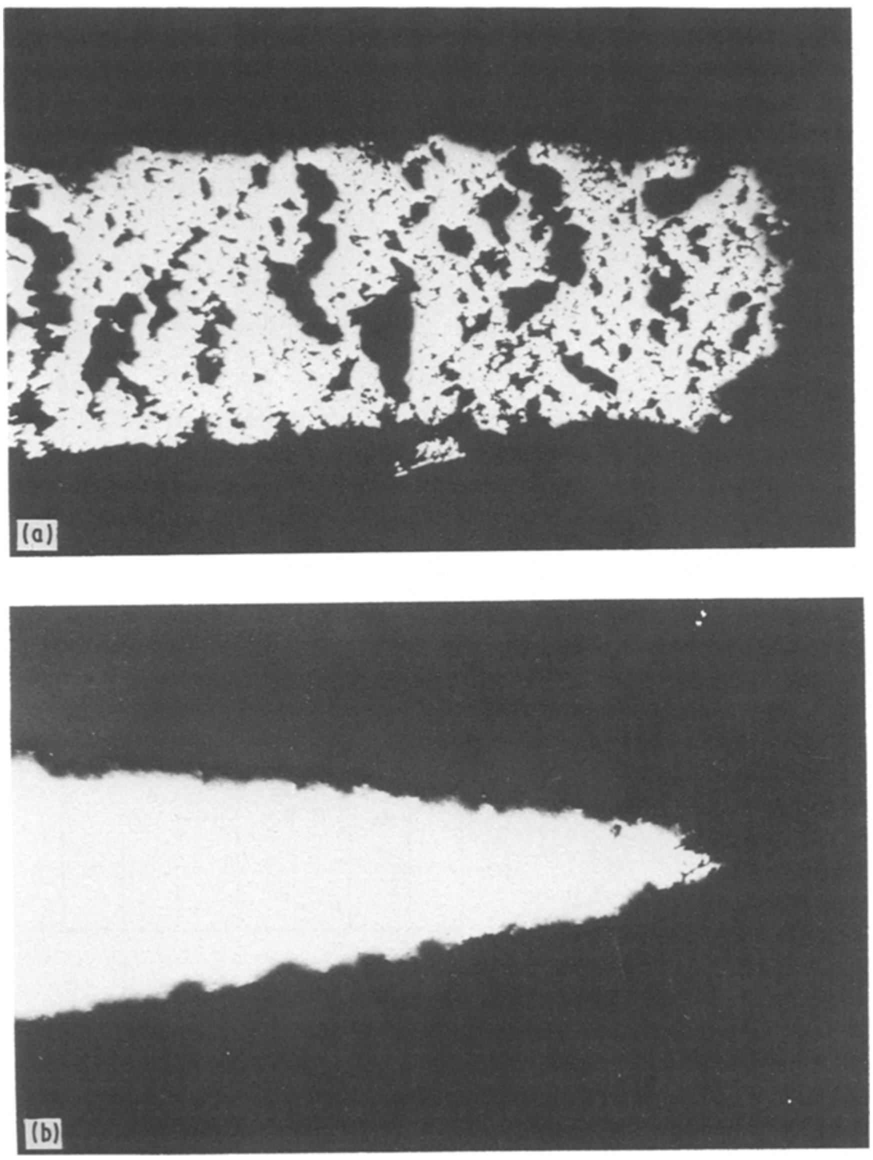

Figure 7 Optical photomicrographs of the fracture tips of specimens of (a) Cu–Zn–Co and (b) Cu–Zn–Cr alloys pulled to fracture at 785° C at an initial strain rate of $10^{-3}\,sec^{-1}$. Tensile axis is horizontal. ×15.

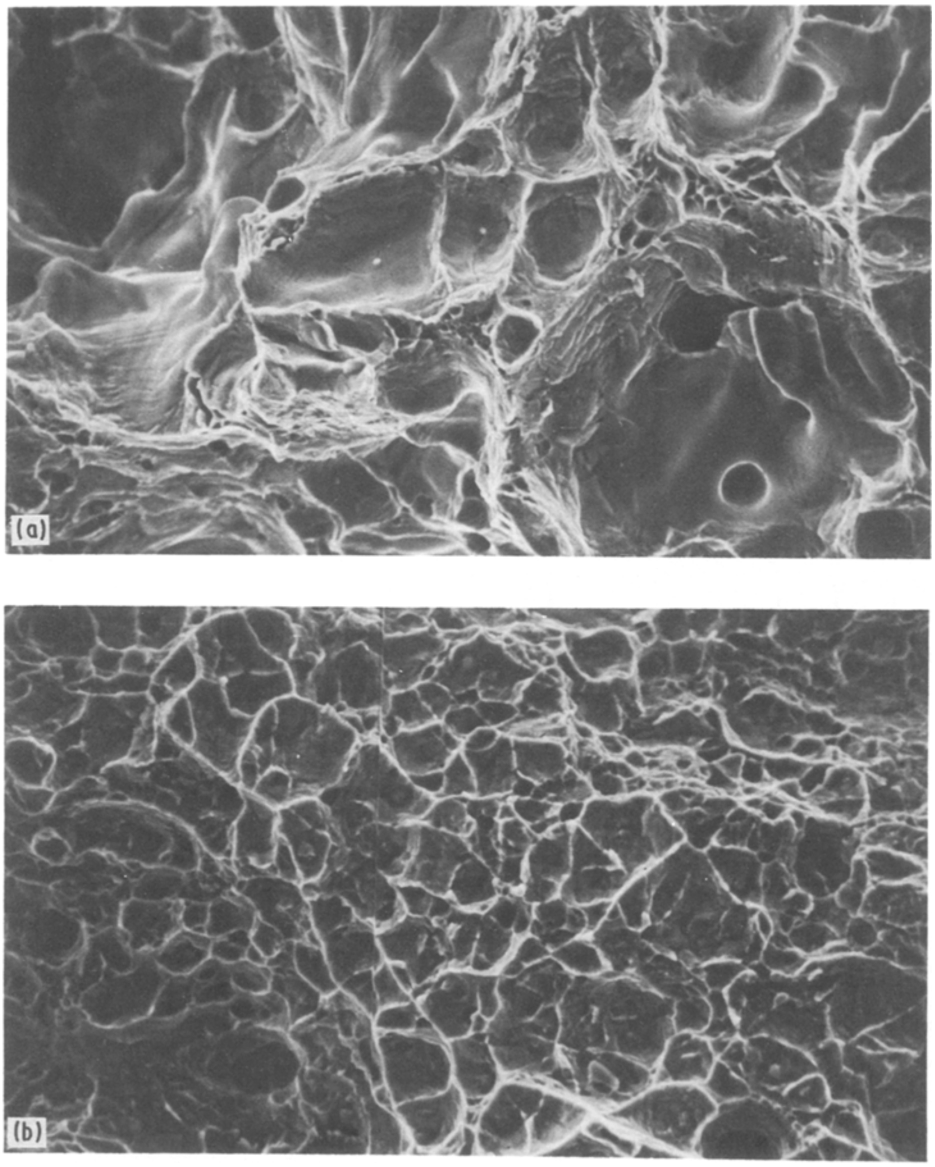

Figure 8 Scanning electron micrographs of the fracture surfaces of specimens of (a) Cu–Zn–Co and (b) Cu–Zn–Cr pulled to failure at 785° C at an initial strain rate of 10^{-3} sec^{-1}. ×550.

present in the alloy are often associated with cavities. Similar observations have also been made by Sagat and Taplin [8] in α/β brass containing 3% Fe. The cavities are essentially uniformly distributed, and appear to grow and interlink by both diffusion and deformation processes [9–11]. Failure occurs because, although there is no visible external necking, the high degree of cavitation including extensive interlinkage reduces very much the effective cross-sectional area.

The present results suggest that fracture of Cu–Zn–Cr specimens in Region II ultimately occur by necking (Fig. 2). The fracture tip of the specimen strained to maximum elongation showed no evidence of void growth and interlinkage. Although the number of voids increased with strain in this alloy, the total area fraction of voids was found to be less than 1% (Fig. 6) even in a specimen which failed with a maximum elongation of 200%, suggesting that cavity growth was restricted in Cu–Zn–Cr alloy. Chandra *et al.* [12] have reported that the high value of strain-rate sensitivity m inhibits internal necking between adjacent voids, thus restricting their growth. It has been found in this work that m decreased from 0.45 to 0.23 during straining in Region II at 785° C and this is attributable primarily to grain coarsening and to a lesser extent to formation of internal voids. The scanning micrographs of the fracture surfaces of this alloy do indicate a coarsening of the microstructure and less evidence of many voids. Any microstructural coarsening destroys the superplastic properties of a material by reducing the strain-rate sensitivity, and so a higher flow stress is needed for further deformation. This situation results in further deformation being confined to the necked region of the specimen, which eventually leads to failure by necking.

It is envisaged that the significant differnce in cavitation behaviour in Cu–Zn–Co and Cu–Zn–Cr alloys in Region II of superplastic flow observed in the present investigation could be the result of various combinations of nucleation and growth stages, the latter being determined by sliding, vacancy condensation and accommodation processes.

5. Conclusions

1. Experiments on the superplastic Cu–Zn–Co and Cu–Zn–Cr alloys show that there are significant

differences in their fracture behaviour, even though both possess similar tensile ductility in Region II. The deformation is quasi-uniform in Cu–Zn–Co alloy and necking appears to be diffuse rather than localized, whereas the Cu–Zn–Cr alloy shows macroscopic necking at very low strains and the final failure occurs by localized neck formation.

2. There is a very extensive cavity formation in Region II in Cu–Zn–Co alloy. The growth and interlinkage of cavities is of major significance in limiting the ductility in this alloy and fracture is due to cavitation failure. On the other hand, a very few and small cavities are observed in Cu–Zn–Cr specimens in Region II and there is no evidence of significant cavity growth and interlinkage even at failure strain, and final failure appears to be due to localized neck formation.

3. The strain-rate sensitivity of flow stress decreases gradually with deformation in Region II in both alloy systems, and this is attributed primarily to microstructural coarsening and to a lesser extent to internal cavity formation.

References

1. G. L. DUNLOP and D. M. R. TAPLIN, *J. Austral. Inst. Metals* **16** (1971) 195.
2. C. W. HUMPHRIES and N. RIDLEY, *J. Mater. Sci.* **9** (1974) 1429.
3. R. D. SCHELLING and G. H. REYNOLDS, *Met. Trans.* **4** (1973) 2199.
4. G. L. DUNLOP, E. SHAPIRO, D. M. R. TAPLIN and J. CRANE, *ibid.* **4** (1973) 2039.
5. T. CHANDRA and I. UEBEL, in Proceedings of International Conference on Creep and Fatigue of Engineering Materials, Swansea, UK, 1973, p. 277.
6. E. E. UNDERWOOD, in "Quantitative Microscopy", edited by R. T. DeHoff and F. N. Rhines (McGraw-Hill, New York, 1986) p. 151.
7. R. G. FLECK, C. J. BEEVERS and D. M. R. TAPLIN, *J. Mater. Sci.* **9** (1974) 1737.
8. G. SAGAT and D. M. R. TAPLIN, *Acta Metall.* **24** (1976) 307.
9. W. BEERE and M. U. SPEIGHT, *Met. Sci.* **12** (1978) 172.
10. I. W. CHEN and A. S. ARGON, *Acta Metall.* **29** (1981) 1759.
11. A. NEEDLEMAN and J. R. RICE, *ibid.* **28** (1980) 1315.
12. T. CHANDRA, J. J. JONAS and D. M. R. TAPLIN, *J. Austral. Inst. Met.* **20** (1975) 220.

Received 23 October 1987
and accepted 23 February 1988